



**HAL**  
open science

## Matching Evaluation of Highly Coupled Dipoles Quantified by a Statistical Approach

Imad Adjali, Ayichatou Gueye, Shermila Mostarshedi, Benoit Poussot,  
Florence Nadal, Jean-Marc Laheurte

► **To cite this version:**

Imad Adjali, Ayichatou Gueye, Shermila Mostarshedi, Benoit Poussot, Florence Nadal, et al.. Matching Evaluation of Highly Coupled Dipoles Quantified by a Statistical Approach. *IEEE Transactions on Antennas and Propagation*, 2020, pp.1-1. 10.1109/TAP.2020.2977753 . hal-02612855

**HAL Id: hal-02612855**

**<https://hal.science/hal-02612855>**

Submitted on 13 Feb 2024

**HAL** is a multi-disciplinary open access archive for the deposit and dissemination of scientific research documents, whether they are published or not. The documents may come from teaching and research institutions in France or abroad, or from public or private research centers.

L'archive ouverte pluridisciplinaire **HAL**, est destinée au dépôt et à la diffusion de documents scientifiques de niveau recherche, publiés ou non, émanant des établissements d'enseignement et de recherche français ou étrangers, des laboratoires publics ou privés.

**What is the problem being addressed by the manuscript and why is it important to the Antennas & Propagation community?**

This paper investigates the effects of electromagnetic coupling between randomly distributed dipoles on their matching properties from a statistical point of view. The well-established UHF RFID may be used in a context of high densities of tags. The proximity of tags can result in an important electromagnetic coupling between tags which alters antenna's key parameters (e.g. radiation pattern and matching). Consequently the quality of communication between the RFID reader and the tags will be degraded. The statistical study of coupling effects can help the RFID engineer to maintain the link quality even in a context of high density of tags.

**What is the novelty of your work over the existing work?**

A pure deterministic modelling of tag behaviour in random configurations would not be realistic. Although intensive research on mutual coupling is available in literature, the impact of the mutual coupling for high densities of RFID tags has never been modelled statistically. This work presents the matching evaluation of dipoles from a statistical point of view. The novelty is to be able to predict the matching properties of a set of random dipoles by their density. Combined to a future study on radiation pattern, this method offers the possibility to express the RFID system parameters (e.g. read-range) statistically.

**Provide up to three references, published or under review, (journal papers, conference papers, technical reports, etc.) done by the authors/coauthors that are closest to the present work. Upload them as supporting documents if they are under review or not available in the public domain.**

- [13] I. Adjali, A. Gueye, B. Poussot, S. Mostarshedi, F. Nadal and J.-M. Laheurte, "Statistical study of coupling in randomly distributed dipole Sets," *12th European Conference on Antennas and Propagation (EuCAP), London, 2018*.

**Provide up to three references (journal papers, conference papers, technical reports, etc.) done by other authors that are most important to the present work**

- [6] G. Marrocco, "RFID grids: Part I—Electromagnetic theory", *IEEE Transactions on Antennas and Propagation*, vol. 59, no.3, pp. 1019-1026, 2011.
- [10] H. King, "Mutual impedance of unequal length antennas in echelon," *IEEE Transactions on Antennas and Propagation*, vol. 5, no. 3, pp. 306-313, 1957.
- [11] H. Baker and A. LaGrone, "Digital computation of the mutual impedance between thin dipoles," *IRE Transactions on Antennas and Propagation*, vol. 10, no. 2, pp. 172-178, 1962.

# Matching Evaluation of Highly Coupled Dipoles Quantified by a Statistical Approach

Imad Adjali, Ayichatou Gueye, Shermila Mostarshedi, Benoit Poussot, Florence Nadal and Jean-Marc Laheurte

**Abstract**— Electromagnetic coupling between randomly distributed dipole antennas is analyzed statistically. The impedance matrix of a set of dipoles is first calculated with both the Induced Electromotive Force (IEMF) technique and Numerical Electromagnetic Code (NEC) simulator. Then, the input impedance of a surrounded dipole is assessed for any loading of the surrounding dipoles. Cumulative distributed functions for the mismatch of a surrounded dipole are given for different dipole densities and loadings of the surrounding dipoles. This statistical approach is proposed in the context of UHF Radio Frequency Identification (RFID) use cases where tag antennas are concentrated in reduced volumes and where the antenna group behavior should be considered.

**Index Terms**—electromagnetic coupling, highly coupled dipoles, impedance matrix, RFID antenna matching

## I. INTRODUCTION

UHF RFID (Radio Frequency Identification) technologies have a long established role for tracking and identification in various fields of application such as food traceability [1], logistics management in textile industry [2] or supply chain management [3]. For instance, UHF RFID tags installed into hotel and hospital linens, towels, uniforms and medical gowns allow for the real-time management and tracking of the laundry activity. This use case is characterized by huge concentrations of tagged items in reduced volumes during the shipping, the storage and the washing steps. Other use cases can be found in the shoe or clothing retail where items can be stacked or aligned yielding to high densities of RFID tags. High density of tags can give rise to an important electromagnetic coupling between tag antennas which alters antenna's key parameters such as the radiation pattern and the matching properties. The decrease in antenna performance ultimately degrades the RFID system performances, e.g. the read range and the read rate of tags. The empirical strategies which are currently proposed rely on either a multiplication of the number of reading systems to bring diversity [4] or a modification in the tags' environment by using mechanical vibration or electromagnetic stirring [5]. The implementation of these solutions results in a heavy and costly infrastructure which is not suitable for large scale applicability of RFID systems and does not guarantee a total reliability.

Manuscript received October 2018.

I. Adjali, A. Gueye, S. Mostarshedi, B. Poussot and J.-M. Laheurte are with Université Paris-Est, ESYCOM (FRE2028), CNAM, CNRS, ESIEE Paris, Université Paris-Est Marne-la-Vallée, F-77454 Marne-la-Vallée, France (phone: +33160957160; e-mail: imad.adjali@u-pem.fr).

F. Nadal is with Université Paris-Est, ESYCOM (FRE2028), CNAM, CNRS, ESIEE Paris, ESIEE Paris, 93162 Noisy-le-Grand, France.

Color versions of one or more of the figures in this communication are available online at <http://ieeexplore.ieee.org>.

Digital Object Identifier AP1810-1949

A solution to optimize the RFID infrastructure may reside in a better understanding and a fine modeling of coupling effects but obviously in such a complex random context, a purely deterministic approach is not appropriate. Although intensive research on mutual coupling [6] has been conducted for over fifty years, the impact of the mutual coupling for high densities of RFID tags has never been modeled statistically to predict their group behavior. By using a more rigorous statistical analysis, our motivation is to build the preliminary version of a statistical tool dedicated to the performance evaluation of any design of tag antenna for a given density of randomly distributed tags. This statistical tool will also be used to optimize the number and positions of the reader's antennas.

In this paper, we assume that the electromagnetic interactions observed in a set of randomly distributed commercial tags built around dipole-like antennas are statistically similar to those of straight dipole antennas. Under this assumption, the driven dipole antenna corresponding to the activated (or read) tag is mismatched by the presence of surrounding dipoles corresponding to neighboring unactivated tags. This paper aims at studying statistically the mismatch of the driven dipole antenna surrounded by a randomly distributed set of dipoles. The other consequence of the antenna coupling, i.e. the distortion of the radiation pattern, is not treated in this paper.

The core of the electromagnetic simulation should present two important characteristics. First, the method should estimate the input impedance of a randomly oriented dipole including mutual coupling with randomly distributed loaded surrounding dipoles. Secondly, the method needs to be fast enough to process a large number of random samples. In this paper, we use the Induced ElectroMotive Force (IEMF) technique [7]–[13] which is a simple analytical method to estimate the self and mutual impedances of two electrically thin dipoles including coupling effects. The technique needs to be extended to the case of a set of randomly oriented thin dipoles. Other analytical or numerical techniques, such as in [14]–[15] can also be used but only for non-inclined dipoles.

The manuscript is organized as follows: in Section II the impedance matrix for two randomly oriented thin dipoles is derived using the IEMF technique and this technique is extended to a set of  $N$  thin dipoles. The Numerical Electromagnetics Code (NEC) [16] is used as a validation reference. In Section III, expressions of the input impedance and the input reflection coefficient are given for a dipole with surrounding dipoles arbitrarily loaded. Then, NEC simulations for isolated and surrounded antennas are compared to IEMF for thin dipoles and to measurements for thick dipoles. In Section IV, NEC and IEMF are both applied

to perform statistical studies of the mismatch of a dipole as a function of the density and the loadings of the surrounding dipoles.

## II. EXTENDED IEMF AND IMPEDANCE MATRIX

The IEMF (Induced ElectroMotive Force) method was introduced by Brillouin in 1922 [7]. This method is based on power conservation, which allows calculating the self-impedance of a small antenna (loop, dipole) with uniform current distribution. In 1929, Pstolkors developed this method in order to calculate the self and mutual resistances of half-wave dipoles [8]. In 1941, Schelkunoff showed that the IEMF method may be used to calculate the self-reactance of dipoles [9]. Later, the IEMF method was used by King [10] to calculate the mutual impedance between staggered parallel antennas of arbitrary length and Baker [11] presented the integral form of the IEMF method for a V shape configuration of dipoles, to be evaluated numerically. In all cases, the self and mutual impedances are obtained supposing a known current distribution (e.g. sinusoidal) on the dipoles. For a few configurations, the expressions of the mutual resistance and reactance are in terms of sine and cosine integrals and can be obtained analytically, for others the evaluation remains numerical.

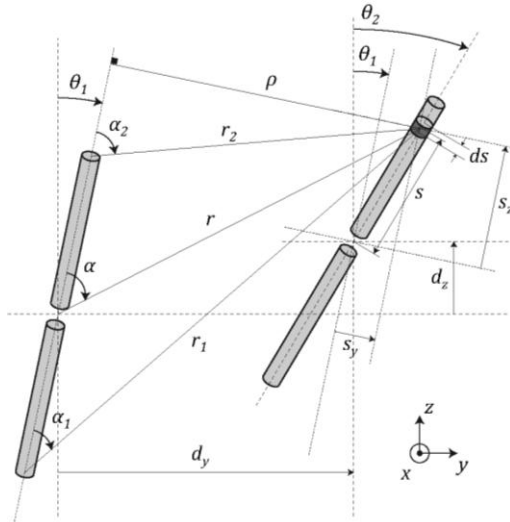


Fig. 1. Two staggered arbitrarily oriented thin dipoles in zOy plane.

Here we consider two staggered arbitrarily oriented dipole antennas of length  $l$  and diameter  $a$  as presented in Fig. 1. The center of the dipoles are situated at  $(y_{01}, z_{01})$  and  $(y_{02}, z_{02})$  and their inclination angles with respect to  $z$  axis are noted  $\theta_1$  and  $\theta_2$  respectively for dipole 1 and 2. If both antennas are considered to be infinitely thin (diameter  $\ll 10^{-3} \lambda$ ) [12], the current distribution on the dipoles can be assumed to be sinusoidal. The self and mutual impedances can thus be calculated by applying the IEMF method. The expressions of the self impedance as presented in [12] are given below:

$$R_{11} = \frac{\eta}{2\pi \sin^2\left(\frac{\beta l}{2}\right)} \left\{ C + \ln(\beta l) - C_i(\beta l) + \frac{1}{2} \sin(\beta l) [S_i(2\beta l) - 2 S_i(\beta l)] + \frac{1}{2} \cos(\beta l) [C + \ln(\beta l/2) + C_i(2\beta l) - 2 C_i(\beta l)] \right\} \quad (1)$$

$$X_{11} = \frac{\eta}{4\pi \sin^2\left(\frac{\beta l}{2}\right)} \left\{ 2 S_i(\beta l) + \cos(\beta l) [2 S_i(\beta l) - S_i(2\beta l)] - \sin(\beta l) \left[ 2 C_i(\beta l) - C_i(2\beta l) - C_i\left(\frac{2\beta a^2}{l}\right) \right] \right\} \quad (2)$$

where  $\eta$  is the characteristic impedance of the medium,  $C_i(x)$  and  $S_i(x)$  are the cosine and sine integrals respectively,  $C = 0.5772$  is the Euler's constant and  $\beta$  is the wave number. For the mutual impedance, we use the expressions presented in [11]:

$$Z_{21} = \int_{-\frac{l}{2}}^{\frac{l}{2}} E_{21} \sin\left(\beta\left(\frac{l}{2} - s\right)\right) ds \quad (3)$$

where the distance from the centre of dipole 2 to some point along its axis is called  $s$ .  $E_{21}$  is the electric field radiated by dipole 1 at this point and is given by:

$$E_{21} = \frac{1}{s} (E_\rho s_y + E_z s_z) \quad (4)$$

where:

$$E_\rho = j \frac{\eta I_{01}}{4\pi \rho} \left\{ e^{-j\beta r_1} \cos(\alpha_1) + e^{-j\beta r_2} \cos(\alpha_2) - 2 \cos\left(\frac{\beta l}{2}\right) e^{-j\beta r} \cos(\alpha) \right\} \quad (5)$$

$$E_z = j \frac{\eta I_{01}}{4\pi} \left\{ 2 \frac{e^{-j\beta r}}{r} \cos\left(\frac{\beta l}{2}\right) - \frac{e^{-j\beta r_1}}{r_1} - \frac{e^{-j\beta r_2}}{r_2} \right\} \quad (6)$$

$I_{01}$  denotes the current magnitude over dipole 1. As we have extended the IEMF formulas presented in [11] to any arbitrary position and orientation of a pair of dipoles in a plane [13], the following equations give the new extended geometrical parameters corresponding to Fig. 1 to be inserted in general equations from (4) to (6):

$$s_y = s \sin(\theta_2') \quad (7)$$

$$s_z = s \cos(\theta_2') \quad (8)$$

$$\theta_2' = \theta_2 - \theta_1 \quad (9)$$

$$Y = d_y - d_z \tan(\theta_1) \quad (10)$$

$$d_y = y_{02} - y_{01} \quad (11)$$

$$d_z = z_{02} - z_{01} \quad (12)$$

$$y_2' = Y \cos(\theta_1) \quad (13)$$

$$z_2' = Y \sin(\theta_1) + \frac{d_z}{\cos(\theta_1)} \quad (14)$$

$$\rho = y_2' + s_y \quad (15)$$

$$r^2 = \rho^2 + (z_2' + s_z)^2 \quad (16)$$

$$r_1^2 = \rho^2 + \left( z_2' + s_z + \frac{l}{2} \right)^2 \quad (17)$$

$$r_2^2 = \rho^2 + \left( z_2' + s_z - \frac{l}{2} \right)^2 \quad (18)$$

$$\cos(\alpha) = \frac{\left( \frac{l}{2} \right)^2 + r^2 - r_2^2}{l r} \quad (19)$$

$$\cos(\alpha_1) = \frac{l^2 + r_1^2 - r_2^2}{2 l r_1} \quad (20)$$

$$\cos(\alpha_2) = \frac{l^2 + r_2^2 - r_1^2}{2 l r_2} \quad (21)$$

Using the above formulas for two dipoles, the impedance matrix of a set of thin dipoles can be calculated by the superposition principle. We call this approach "extended IEMF" where the IEMF method is applied for each pair of dipoles in the set. The superposition is valid if adding an extra dipole to a pair of antennas does not alter the previous estimated values of the self and mutual impedances of the pair, thus the condition of minimum scattering is satisfied [17]. In the case of thin dipoles, for which the IEMF method is sufficiently accurate, this condition is not restrictive and results in very small distances.

The extended IEMF method needs to be validated by a reference method for two reasons. First, the IEMF method is here applied to an arbitrary position and orientation of two dipoles. Secondly, the IEMF method has originally been developed for two dipoles and here it is extended to a set of dipoles. The extended IEMF for a set of half-wave thin dipoles is validated for two configurations by a comparison with Numerical Electromagnetics Code (NEC) which is a popular simulator for wire antennas based on Method of Moments. This simulator is relatively fast and can be easily automated in order to generate the necessary database for statistical studies. The frequency under consideration is 892 MHz which corresponds to the medium frequency between the European and US UHF RFID bands. In this paper  $\lambda$  corresponds to the wavelength calculated at this frequency.

#### A. 1D Set of Randomly Distributed Parallel Dipoles

A randomly distributed set of 10 thin identical parallel dipoles of diameter  $10^{-6} \lambda$  is considered (see Fig. 2). The dipole centers are distributed randomly in one dimension. The diagonal elements of the  $N \times N$  impedance matrix are equal to the self-impedance ( $Z_{ii}$ ) of a single dipole. The mutual impedances  $Z_{ij} = Z_{ji}$  are obtained for any pair ( $i, j$ ) of dipole in the array in the absence of the other dipoles. The results are compared to NEC simulations and the absolute error on each element of the matrix is shown in Fig. 3 where the axes correspond to the dipole index (from 1 to 10). Unlike the extended IEMF technique, NEC takes the interactions between all dipoles into account.

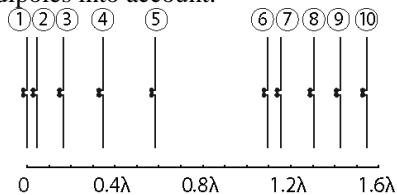


Fig. 2. Random distribution of 10 thin dipoles over a  $1.6\lambda$  length.

As shown in Fig. 3, the absolute error values on the real and imaginary parts of the impedance are limited to a maximum of  $7 \Omega$ .

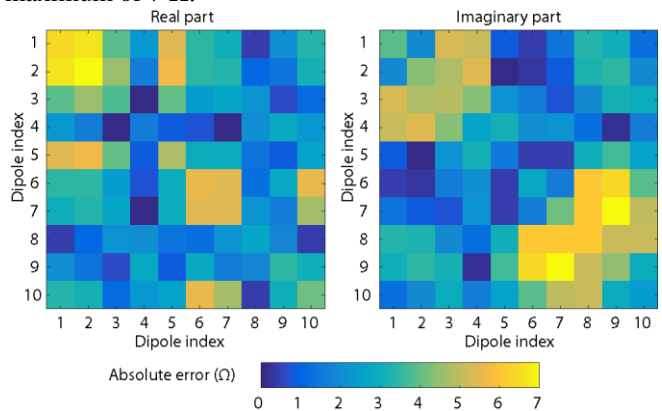


Fig. 3. Absolute error values in Ohms between the extended IEMF and NEC on the real (left) and imaginary (right) parts of the impedance matrix of a randomly distributed set of 10 parallel dipoles.

The core of the NEC code is called by a MATLAB program which allows the automation of the procedure requiring multiple simulations. Fig. 4 depicts the evolution of the computation time of an impedance matrix for both the extended IEMF and NEC as a function of the number of dipoles in the set. The calculation time grows drastically as the number of dipoles in the set increases. This is due to the fact that in NEC, wires are discretized into short segments with linear variations of current and voltage, unlike the IEMF method, where the entire dipole is considered as one segment with a known current distribution. In other words, IEMF has a single complex unknown while NEC deals with  $n$  complex unknowns for  $n$  discretizations. The IEMF method shows consequently lower computation times. In this paper, NEC results have been obtained by discretizing the half-wave dipoles into 51 segments ( $\lambda/100$ ). Fig. 4 shows that in the case of 10 dipoles, the extended IEMF technique is approximately 40 times faster than NEC.

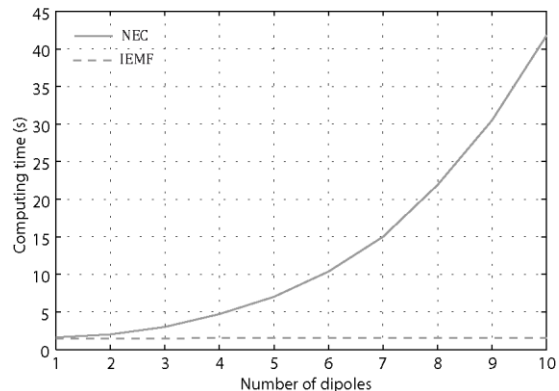


Fig. 4. Computation time of the impedance matrix obtained by the extended IEMF and NEC as a function of the number of dipoles.

#### B. 2D Set of Randomly Distributed Dipoles

A randomly distributed set of 10 thin identical dipoles is presented in Fig. 5. The centers are distributed randomly in two dimensions and each dipole has a random orientation under the condition that dipole overlaps are forbidden. Two distribution areas are considered:  $2\lambda \times 2\lambda$  and  $\lambda \times \lambda$ . The

impedance matrix of each set has been calculated as previously explained and the result has been compared to the matrix provided by NEC. The absolute error on the real and imaginary parts of the impedance for each element of the matrix is shown in Fig. 6. The maximum absolute error is limited to  $9.3 \Omega$  and is observed for the highest antenna density.

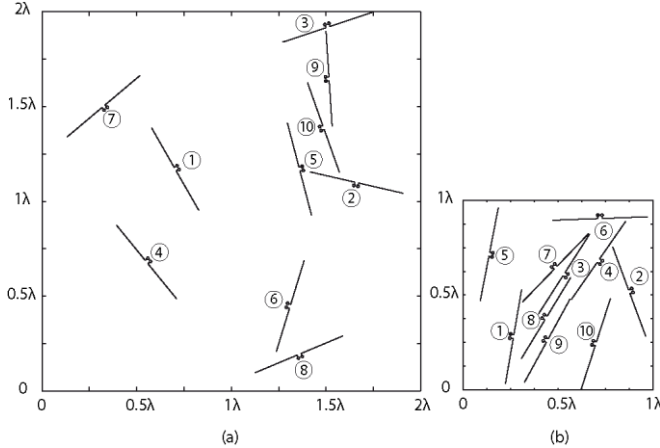


Fig. 5. Random distribution of 10 thin dipoles over two dimensions for two different distribution areas (a)  $2\lambda \times 2\lambda$  and (b)  $\lambda \times \lambda$ .

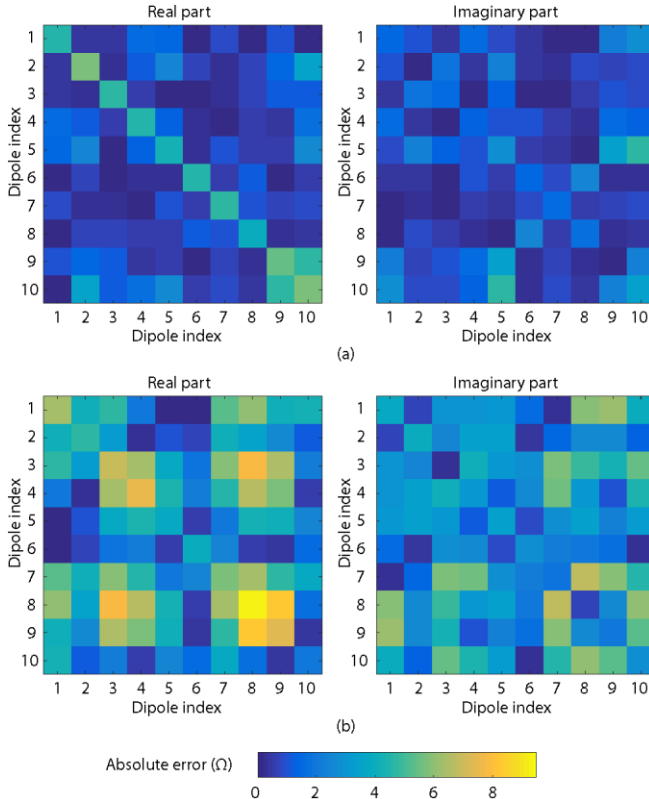


Fig. 6. Absolute error values in Ohms between the extended IEMF and NEC on the real (left) and imaginary (right) parts of the impedance matrix for a randomly distributed set of 10 dipoles and for two different distribution areas (a)  $2\lambda \times 2\lambda$  and (b)  $\lambda \times \lambda$ .

It is not pertinent to calculate a relative error in this phase because an insignificant error on a low impedance of a matrix element can result in a very high relative error. We will

present relative error values for the parameters of interest, i.e. the input impedance of each driven dipole.

### III. INPUT IMPEDANCE OF A DRIVEN DIPOLE SURROUNDED BY LOADED DIPOLES

The input impedance of a driven dipole surrounded by loaded dipoles is calculated by using the equivalent  $N$ -port network presented in Fig. 7.

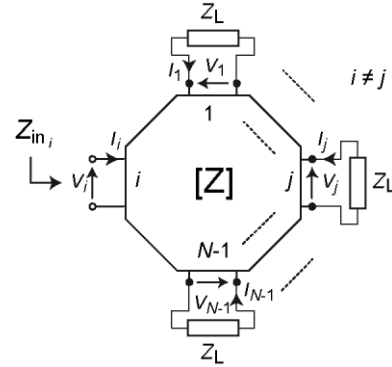


Fig. 7. Input impedance of a loaded  $N$ -port network.

The input impedance at port  $i$  is calculated when all the  $(N-1)$  other ports are loaded with  $Z_L$ . Knowing that the general  $Z$  matrix definition leads to  $[V] = [Z][I]$  and that for each loaded port  $V_j = -Z_L I_j$ , the input impedance at port  $i$  defined by  $Z_{in\ i} = V_i / I_i$  is given by:

$$Z_{in\ i} = \frac{1}{Z_{mod\ ii}^{-1}(i,i)} \quad (22)$$

where  $Z_{mod\ ii}^{-1}$  is the inverse of the  $N \times N$  matrix obtained by adding  $Z_L$  to the main diagonal of the general  $Z$  matrix of the network everywhere except on the  $(i, i)^{th}$  element:

$$Z_{mod\ ii} = \begin{bmatrix} Z_{11} + Z_L & \dots & Z_{1i} & \dots & Z_{1N} \\ \dots & \dots & \dots & \dots & \dots \\ Z_{i1} & \dots & Z_{ii} & \dots & Z_{iN} \\ \dots & \dots & \dots & \dots & \dots \\ Z_{N1} & \dots & Z_{Ni} & \dots & Z_{NN} + Z_L \end{bmatrix} \quad (23)$$

It can be experimentally shown that for physical loads ( $Z_L$  presenting a positive real part), this matrix is always invertible.

It is important to notice that the absolute errors on the impedance matrices of Fig. 3, Fig. 6 (a) and Fig. 6 (b) result in a relative error on  $Z_{in}$  between NEC and extended IEMF defined as  $\left| \frac{Z_{in\ IEMF} - Z_{in\ NEC}}{Z_{in\ NEC}} \right|$ . The maximum of the absolute value of this error observed for one driven dipole among 10 is equal to 4% for Fig. 2, 4.3% for Fig. 5 (a) and 25% for Fig. 5 (b). In Section IV, we will focus on the statistical matching behavior of the dipoles where those errors will prove to have no influence on the general statistical conclusions. The two following subsections present an experimental validation of  $Z_{in}$  for the isolated and surrounding dipoles over a large frequency band.

#### A. Isolated Dipole

The input impedance of a thin isolated dipole of length 17 cm ( $\approx 0.5 \lambda$ ) and diameter  $0.3 \mu\text{m}$  ( $\approx 10^{-6} \lambda$ ) has been calculated by IEMF and compared to NEC. The input

impedance of a thick isolated dipole of length 17 cm and diameter 1 mm has also been calculated by NEC and compared to measurements.

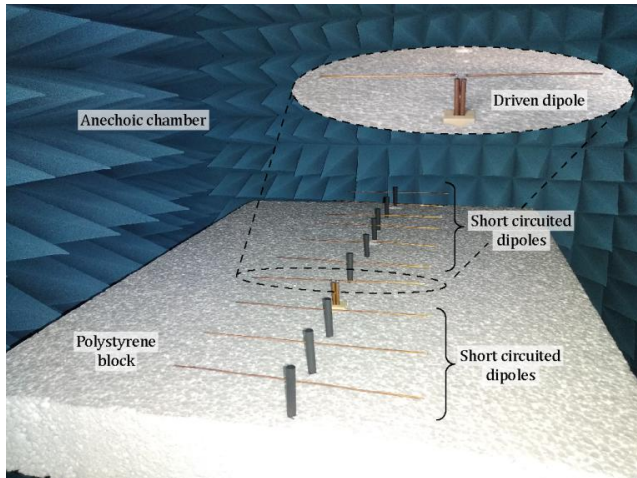


Fig. 8. Experimental setup for the impedance measurement of a random distribution of 10 thick dipoles in anechoic chamber (one driven dipole and nine surrounding short-circuited dipoles).

As shown in Fig. 8, the measurements have been performed in the anechoic environment of the Voyantic Cabinet [18] used to determine the radiation pattern of UHF RFID tags. Thick dipoles have been fabricated with copper wires and fixed to a block of polystyrene whose relative permittivity is close to 1. The driven element has been fed differentially by a 2-port Vector Network Analyzer (VNA).

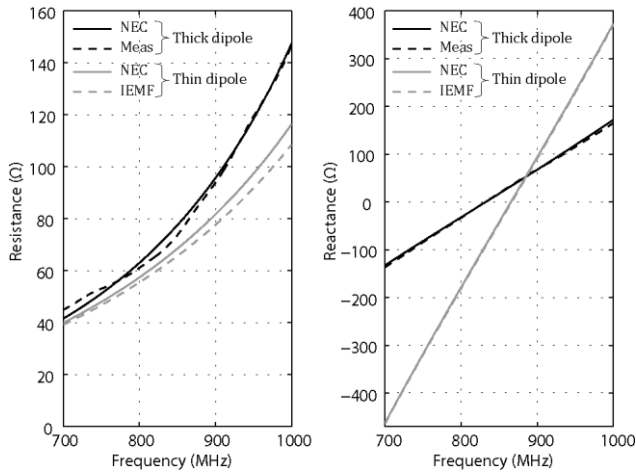


Fig. 9. Input impedance of an isolated thin and thick dipole.

The input impedance of the driven element is finally extracted from the measured [S] matrix using the procedure described in [19]. Fig. 9 presents the real and imaginary parts of the input impedance as a function of the frequency. NEC results for both thin and thick dipoles are in excellent agreement with IEMF and measurements, respectively. This confirms that NEC can be used as a reference code for both thin and thick cases as measurements are not easy to carry out for extremely thin dipoles and IEMF accuracy is limited for thick dipoles.

B. Surrounded Dipole

For the randomly distributed dipoles (1D or 2D) presented in Fig. 2 and Fig. 5, the input impedance is calculated for different driven dipoles. Fig. 10 depicts the input impedance of the driven dipole (either dipole n°1 or n°7) in the parallel configuration (Fig. 2) as a function of the frequency in the case of thin or thick dipoles. Surrounding dipoles are short-circuited. The results not only prove the validity of the procedure (NEC compared to extended IEMF for thin dipoles and to measurement for thick dipoles) but also show a high dispersion of the input impedance in a random configuration. Consequently, each surrounded dipole might be highly mismatched or not according to its position in a random configuration.

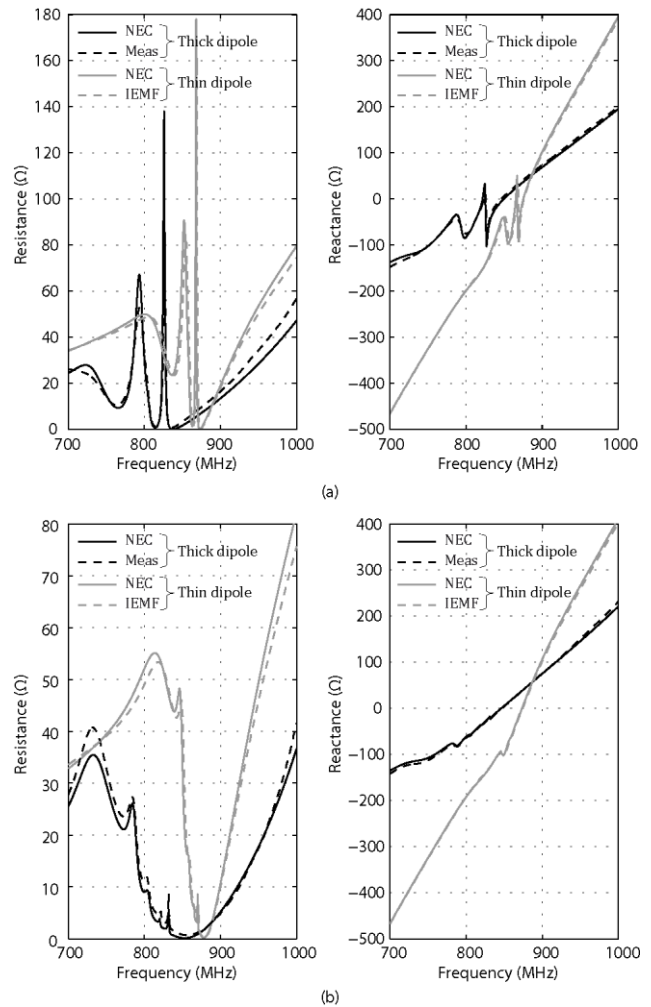


Fig. 10. Input impedance of dipole (a) n°1 and (b) n°7 in the set of randomly distributed parallel dipoles (Fig. 2).

Two other dipoles have been chosen in the considered 2D randomly distributed sets (Fig. 5) and the results are shown in Fig. 11. We observe more fluctuations of the real and imaginary parts in the case of the highest density of dipoles (Fig. 11.b).

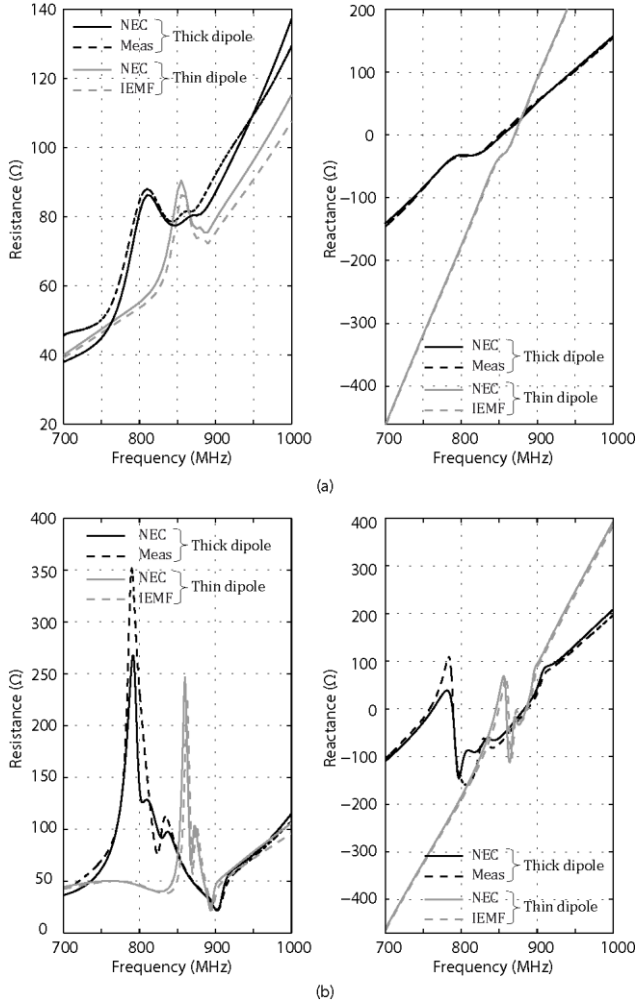


Fig. 11. Input impedance of a dipole in the set of randomly distributed dipoles for different distribution areas (a) dipole n°5 in  $2\lambda \times 2\lambda$  (Fig. 5.a) and (b) dipole n°1 in  $\lambda \times \lambda$  (Fig. 5.b).

IV. STATISTICAL ASSESSMENT

This section is dedicated to the statistical assessment of the mismatch for a surrounded dipole in different random configurations. To this end, we define the reflection coefficient  $\Gamma_{in i}$  for the  $i^{th}$  surrounded dipole as follows:

$$\Gamma_{in i} = \frac{Z_{in i} - Z_{ref}^*}{Z_{in i} + Z_{ref}} \quad (24)$$

where the reference impedance  $Z_{ref}$  is chosen to be the complex conjugate of the self-impedance of an isolated dipole. The self-impedance of an isolated thin dipole of diameter  $0.3 \mu\text{m}$  is calculated by extended IEMF and NEC:  $Z_{self\_thin\_IEMF} = 77.6 + j91 \Omega$  and  $Z_{self\_thin\_NEC} = 81.7 + j93.59 \Omega$ . The self-impedance of an isolated thick dipole of diameter  $1 \text{mm}$  is obtained by measurements and NEC:  $Z_{self\_thick\_meas} = 93.93 + j68.09 \Omega$  and  $Z_{self\_thick\_NEC} = 95.65 + j67.55 \Omega$ . The statistical studies are conducted through two different axes: the reflection coefficient and the bandwidth of surrounded dipoles.

A. Reflection Coefficient

Ten identical dipoles are randomly distributed over surfaces of dimensions  $4\lambda \times 4\lambda$ ,  $3\lambda \times 3\lambda$ ,  $2\lambda \times 2\lambda$  and  $1\lambda \times 1\lambda$ , i.e.

using four different densities. For each dipole density, 200 random configurations have been generated with thin and thick dipoles. The magnitude of the input reflection coefficient ( $\Gamma_{in}$ ) for each of the 10 dipoles has been calculated in dB when all other dipoles are either short-circuited or matched. Therefore,  $200 \times 10 = 2000$  samples are available for each dipole density. The cumulative distribution functions (CDF) are presented in Fig. 12.

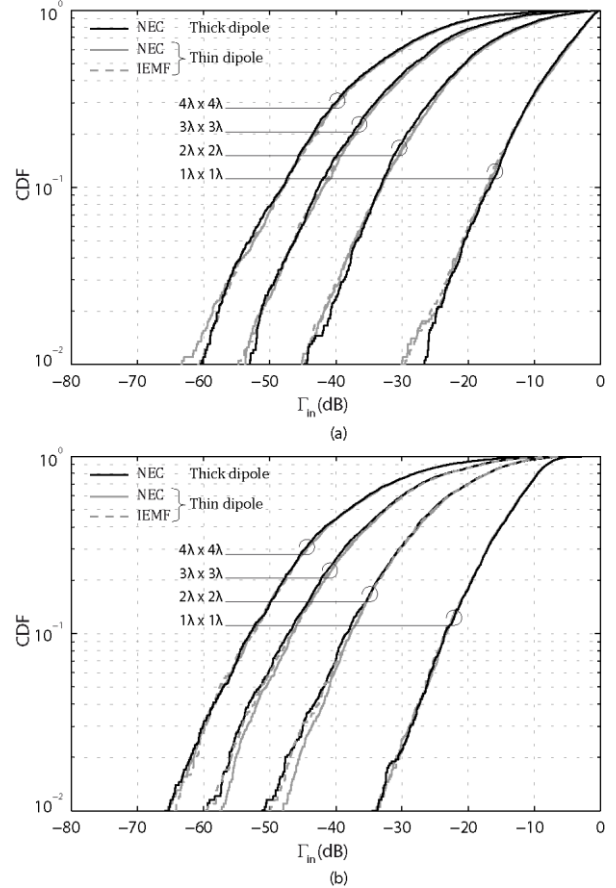


Fig. 12. Cumulative distribution functions of the input reflection coefficient of a dipole, surrounded by (a) short-circuited dipoles and (b) matched dipoles, as a function of the densities obtained by extended IEMF (thin dipoles) and NEC (thin and thick dipoles).

An excellent agreement is observed between the three series of CDF obtained by extended IEMF and NEC. This figure leads to an important conclusion: the statistical behavior of thick and thin dipoles is similar even if the intrinsic values of their input impedances and thus the reflection coefficients are quite different. For both loadings and for a given mismatch level, the number of dipoles presenting better matching properties increases as the distribution surface increases (or the dipole density decreases). In the case of short-circuited surrounding dipoles, the percentage of dipoles presenting a reflection coefficient smaller than  $|\Gamma_{in}| = -10 \text{ dB}$ , is equal to 33% for the highest density ( $1\lambda \times 1\lambda$ ) and reaches 97.5% for the lowest density ( $4\lambda \times 4\lambda$ ). Finally, the loads of the surrounding dipoles have an important influence on the input reflection coefficient of a surrounded dipole. We observe that for a given dipole density,

the percentage of mismatched antennas decreases if the surrounding dipoles are terminated by a matched load compared to the case when they are short-circuited. For the highest dipole density ( $1\lambda \times 1\lambda$ ), the percentage of dipoles presenting a reflection coefficient better than  $|\Gamma_{in}| = -10$  dB increases from 33% with short-circuited surrounding dipoles to 77% with matched surrounding dipoles. This result can be physically explained by the higher radar cross-section of short-circuited dipoles compared to matched dipoles yielding a higher backscattering and a higher disturbance on the driven dipole. It must be mentioned that RFID tag antennas are normally designed to be matched to the RFID chip impedance when the tag is unactivated. Therefore, the matched configuration of surrounding dipoles can be associated to a realistic RFID scenario. However, despite these statistical results, it is not yet possible to conclude on the read rate of the RFID tags, without studying the impact of the mutual coupling on the radiation pattern. In other words, the absolute gain of the tag antenna in the reader's direction includes the mismatch of the driven dipole as well as the radiation gain (or directivity) of this latter in that direction. This analysis is however out of the scope of this paper.

Finally, it must be noticed that the relative errors on input impedances between NEC and extended IEMF observed for a few configurations in Section III do not have significant impact on the general conclusions that can be drawn using the statistical results as observed in Fig. 12. Here the statistical behavior of a large number of configurations is considered and the locally high or low errors are of no interest.

**B. Bandwidth**

The typical reflection coefficient of an isolated dipole is plotted as a function of frequency in Fig. 13. For a given threshold of the reflection coefficient, the isolated dipole shows a certain frequency bandwidth. The bandwidth of the isolated dipole is used as a reference in the study of the surrounded dipole.

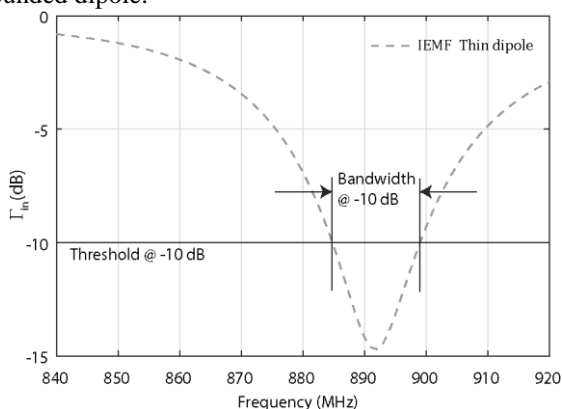


Fig. 13. Reflection coefficient of the isolated thin dipole under study as a function of frequency.

The statistical influence of the neighboring dipoles over the bandwidth of a surrounded dipole is performed using the same scenarios as in the previous subsection. The same number of dipoles is randomly distributed using the four different densities, and 100 random configurations have been generated with thin dipoles with short-circuited neighboring dipoles. For each distribution density and for a fixed threshold

of the reflection coefficient, the percentage of dipoles covering a given desired bandwidth around 892 MHz can be read over the plots of Fig. 14.

For example, the percentage of dipoles satisfying a 3 MHz bandwidth for a -10 dB threshold is equal to 97.1% for a  $4\lambda \times 4\lambda$  distribution surface while the percentage reduces to 68.7% for a  $1\lambda \times 1\lambda$  surface where the coupling effects are more important due to the higher distribution density.

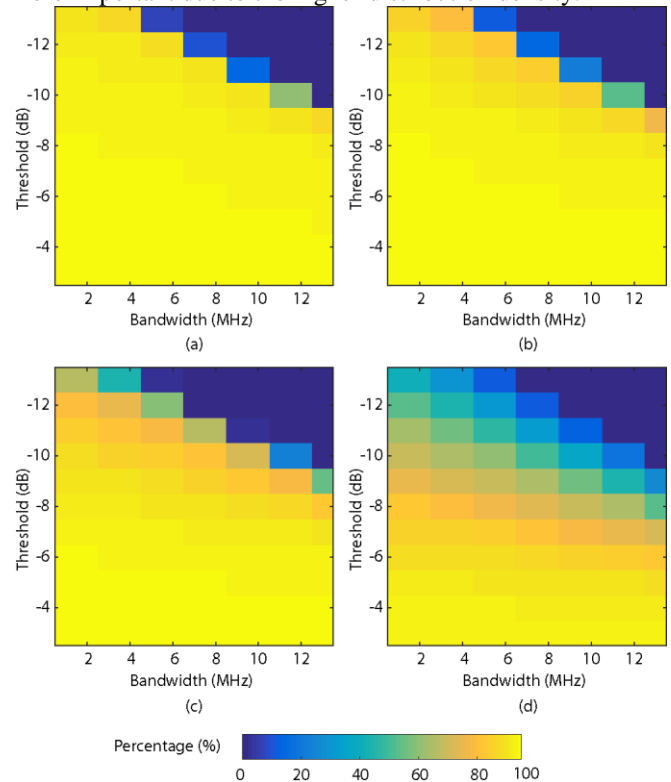


Fig. 14. Percentage of dipoles presenting at least a given bandwidth for a fixed threshold of the reflection coefficient for different distribution densities (a)  $4\lambda \times 4\lambda$ , (b)  $3\lambda \times 3\lambda$ , (c)  $2\lambda \times 2\lambda$  and (d)  $1\lambda \times 1\lambda$ .

**V. CONCLUSION**

A set of RFID tag antennas has been modeled by a set of arbitrarily distributed dipoles where the matching properties of the isolated driven tag are modified by the presence of neighboring dipoles. As the position, orientation and density of the tags in the targeted RFID scenarios are random parameters, a purely deterministic approach cannot describe the coupling phenomena realistically. It has been shown that the impedance matrix of the set, including the coupling effects, can be constructed with the rather fast numerical electromagnetic simulator NEC. For thin dipoles, a purely analytical approach based on the IEMF technique has been used with a considerable saving of computation time. It has also been demonstrated that the statistical behavior of thin dipoles simulated by extended IEMF is similar to those of thick dipoles simulated by NEC.

Our approach clearly allows quantifying the statistical influence of the electromagnetic coupling on the matching for different dipole densities. In on-going works, our approach is extended to statistically assess the radiation pattern distortions. In further developments, instead of a single driven element and surrounding coupled dipoles, our formulation

will consider a plane wave illuminating all dipoles and modeling the reader signal as suggested in [6]. The ultimate objective is to provide a quick NEC-based tool to evaluate the statistical performance of any design of wire antenna in use-cases where high densities of tags are observed. In that sense, this work is the first attempt to handle the group behavior of tag antennas in the UHF RFID context.

#### REFERENCES

- [1] R. S. Chen, C. C. Chen, K. C. Yeh, Y. C. Chen and C. W. Kuo, "Using RFID technology in food produce traceability," *WSEAS Transactions on information science and applications*, vol. 5, no. 11, pp. 1551-1560, 2008.
- [2] A. P. Hum, "Fabric area network—a new wireless communications infrastructure to enable ubiquitous networking and sensing on intelligent clothing," *Computer Networks*, vol. 35, no. 4, pp. 391-399, 2001.
- [3] G. M. Gaukler and R.W. Seifert, "Applications of RFID in supply chains," *Trends in supply chain design and management*, pp. 29-48, Springer London, 2007.
- [4] L. Wang, B. A. Norman, and J. Rajgopal, "Placement of multiple RFID reader antennas to maximise portal read accuracy," *International Journal of Radio Frequency Identification Technology and Applications*, vol. 1, no. 3, p. 260, 2007.
- [5] J. R. Kruest and G. Bann, "Systems and methods for stirring electromagnetic fields and interrogating stationary RFID tags," U.S. Patent No. 7,884,725, 8 Feb. 2011.
- [6] G. Marrocco, "RFID grids: Part I—Electromagnetic theory," *IEEE Transactions on Antennas and Propagation*, vol. 59, no. 3, pp. 1019-1026, 2011.
- [7] L. Brillouin, "Sur l'origine de la résistance de rayonnement," *Radio électricité*, vol. 3, no. 4, pp. 147-152, 1922.
- [8] A. A. Pistorius, "The radiation resistance of beam antennas," *Proc. IRE*, vol. 17, no. 3, pp. 562-519, 1929.
- [9] S. A. Schelkunoff, "Theory of antennas of arbitrary size and shape," *Proc. IRE*, vol. 29, no. 9, pp. 493-521, 1941.
- [10] H. King, "Mutual impedance of unequal length antennas in echelon," *IEEE Transactions on Antennas and Propagation*, vol. 5, no. 3, pp. 306-313, 1957.
- [11] H. Baker and A. LaGrone, "Digital computation of the mutual impedance between thin dipoles," *IRE Transactions on Antennas and Propagation*, vol. 10, no. 2, pp. 172-178, 1962.
- [12] C. A. Balanis, *Antenna theory: analysis and design*, John Wiley & Sons, 2015.
- [13] I. Adjali, A. Gueye, B. Poussot, S. Mostarshedi, F. Nadal and J.-M. Laheurte, "Statistical study of coupling in randomly distributed dipole sets," *12th European Conference on Antennas and Propagation (EuCAP), London, 2018*.
- [14] A. E. Gera, "Simple expressions for mutual impedances," *Inst. Electr. Eng. Proc.*, vol. 135, no. 6, pp. 395-399, 1988.
- [15] H. A. Abdallah and W. Wasylkiwskyj, "A numerical technique for calculating mutual impedance and element patterns of antenna arrays based on the characteristics of an isolated element," *IEEE Trans. Antennas Propag.*, vol. 53, no. 10, 2005.
- [16] G. J. Burke, A. J. Poggio, J. C. Logan and J. W. Rockway, "Numerical Electromagnetic Code (NEC)," *IEEE Int. Symp. Electromagn. Compat.*, San Diego, pp.1-3, 1979.
- [17] A. J. Roscoe and R.A. Perrott, "Large finite array analysis using infinite array data," *IEEE Transactions on Antennas and Propagation*, vol. 42, no.7, pp. 983-992, 1994.
- [18] Tagformance pro, Voyantic Ltd, Espoo, Finland [Online]. Available: [http://voyantic.com/tagformance\\_pro](http://voyantic.com/tagformance_pro)
- [19] K. D. Palmer and M. W. Van Rooyen, "Simple broadband measurements of balanced loads using a network analyzer," *IEEE Trans. On Instrument. & Meas.*, vol. 55, no. 1, pp. 266-272, 2006.
- [20] K. Kurokawa, "Power waves and the scattering matrix," *IEEE Trans. Microw. Theory Tech.*, vol. 13, no. 3, pp. 194-202, 1965.